THE CONFUSION LIMITS TO THE SENSITIVITY OF SUBMILLIMETER TELESCOPES

G. Helou
Infrared Processing and Analysis Center
Jet Propulsion Laboratory, California Institute of Technology

and

C. A. Beichman
Jet Propulsion Laboratory, California Institute of Technology
and
The Institute for Advanced Study

ABSTRACT

Outside of the Galactic plane there are two major sources of confusion that limit the sensitivity of continuum observations at submillimeter wavelengths: the spatial structure of the thermal emission from dust in the Milky Way, and the crowding of extragalactic sources at faint levels. We present estimates of the "noise" expected from these two types of confusion as a function of wavelength and beam size on the sky, and compare them to detector and photon noise estimates for proposed space-borne telescopes. Confusion "noise" cannot be reduced by longer integration times or more sensitive detectors, and can limit the performance of cryogenic telescopes in the one-meter class to a photometric uncertainty between 1 and 10 mJy at $\lambda > 100\mu$m.

Keywords: confusion, galaxy counts, cirrus, telescopes, sensitivity.

1. INTRODUCTION

The sensitivity of a telescope designed for operation at infrared or submillimeter wavelengths is determined by the thermal background of the telescope itself, by detector performance, and ultimately by natural backgrounds. The minimum possible noise due to celestial backgrounds arises in statistical variations in the total photon rate from the sky. However, spatial non-uniformity in that emission can set considerably higher limits to the minimum measurable signals, as it curtails our ability to assign a flux to a position. This effect, generally called "confusion", can be caused either by structure modulating the diffuse celestial background, or by the random distribution of discrete sources.

The confusion limits to sensitivity depend primarily on the size of the beam used for the observations and cannot be reduced by longer integration times. While these limits for a given region of sky can be reduced by optimizing the sky subtraction strategy or sampling at higher spatial frequency, confusion will set a firm boundary to the performance of a telescope.

The diffuse emission from dust in the Galaxy, known as "the infrared cirrus" (Ref. 1) is observed as filaments and clouds across almost the entire sky. The cirrus exhibits however a strong dependence on Galactic latitude, and is quite patchy on the scale of degrees; it is thus possible to minimize confusion by cirrus by avoiding bright areas in *IRAS* 100 μm maps, or in 21 cm maps of neutral hydrogen which correlate well with the infrared cirrus (Ref. 2). The confusion due to extragalactic sources is, however, relatively uniform across the sky; we ignore variations in source counts due to clustering of galaxies.

This paper estimates the confusion noise levels due to cirrus and to source crowding, and compares the results to other noise sources for representative models of various planned or proposed telescopes. All telescopes discussed here are assumed to operate at the diffraction limit at each wavelength λ, with a beam subtending $\Omega_{bm} = 1.6\lambda^2/A$, where A is the collecting area of the primary mirror. Equivalently, the effective beam diameter is $d = 1.6\lambda/D$, where D is the diameter of the primary.

2. CONFUSION BY CIRRUS

The measurement of the brightness of a source involves subtracting the sky background derived from a judiciously chosen reference field. Since the sky is not uniform, the measurement will include a noise component due to difference in the brightness of the sky (smoothed by the telescope beam) between the source and reference positions. The magnitude of the noise associated with cirrus confusion depends on the beam size and configuration used for background subtraction, and on the amount of structure in the cirrus at the spatial frequencies corresponding to the beam size. Gautier *et al.* (Ref. 3) used *IRAS* data at 100 μm to compute the power spectrum P of the spatial fluctuations of cirrus emission as a function of angular frequency r, for angles between 4′ and 400′. They found the data could be well fit by

$$P = P_0(r/r_0)^{\alpha} \qquad (1)$$

with $\alpha \sim -3$ in four different clouds. P_0 scales roughly as the cube of the average surface brightness B_0 of the cirrus cloud, measured on $\sim 1°$ scale. Gautier *et al.* then estimated the statistical errors expected in photometric measurements against a background characterized by a power spectrum of the form in Eq. 1, and assuming either two symmetrically-placed reference apertures or a reference annulus for background subtraction. They found

$$\sigma_{cir} = E_0(d/d_0)^{(1-\frac{\alpha}{2})}P_0^{\frac{1}{2}}, \qquad (2)$$

where d is the beam diameter, and d_0 is the angle at which P_0 is evaluated. E_0 is a function of α, the background subtraction strategy, the beam size, and the distance to reference points (with the last two

Proc. 29th Liège International Astrophysical Colloquium From Ground-Based to Space-Borne Sub-mm Astronomy, Liège, Belgium 3-5 July 1990, ESA SP-314 (December 1990)

angles scaled to λ/D). For telescopes operating at the diffraction limit at 100 μm, and for σ_{cir} in Jy and B_0 in Jy sr^{-1}, the following approximation can be derived from the Gautier *et al.* results:

$$\sigma_{cir} \simeq 2.65 E_0 \left(\frac{\lambda}{D}\right)^{2.5} B_0^{1.5}. \quad (3)$$

In what follows, we adopt a rather efficient scheme for background subtraction, where the reference aperture is an annulus with a width $1.6\lambda/D$ (*i.e.* equal to d) and a radius twice as large, resulting in $E_0 = 1.15\ 10^{-3}$ for our choice of Ω_{bm}. We then extend the use of Eq. 3 to all wavelengths using the cirrus brightness spectrum $B_0(\lambda)$ of Désert *et al* (Ref. 4), which falls off roughly like $\lambda^{-3.2}$ beyond 600 μm. The assumptions underlying this extrapolation are (1) that the power-law scaling in Eq. 1 applies down to a scale of a few arcseconds, (2) that the exponent α in Eq. 1 remains near -3 for wavelengths other than 100 μm, and (3) that the empirical relation of P_0 scaling like B_0^3 also holds at wavelengths other than 100 μm. Given these assumptions, cirrus confusion noise expressed as a flux density per beam scales with telescope diameter as $D^{-2.5}$ at constant λ. At constant D, it rises with increasing λ very steeply (due to the sharp rise of the thermal emission from large, cold grains at short wavelengths), flattens out, then drops again beyond 300 μm, scaling roughly like λ^{-2} at 1 mm.

3. CONFUSION BY GALAXIES

Photometry in the presence of a population of discrete sources can be hampered either by the collective effect of fainter sources which contribute stochastically to the brightness of each resolution element on the sky, or by the presence of an identifiable bright source close to the object of interest. The faint source confusion limit is set by comparing the desired photometric uncertainty with the noise resulting from uneven crowding of faint sources. The bright source confusion limit is determined by comparing the desired completeness of a survey with the frequency with which sources in the survey are expected to overlap to the point where photometric information is lost.

We introduce the counts of extragalactic sources as a function of flux density f_ν and of λ in §3.1, then describe the algorithms used to compute the source confusion noise due to faint and bright sources in §3.2 and 3.3. Results are presented in § 4 as a function of wavelength and telescope size.

3.1. Source Counts

Source counts are estimated by modeling an extragalactic source population characterized by a luminosity function, and by a spectral distribution of the emission from each source. The effects of evolution are discussed below. The sources are taken to have a volume density distribution given by an analytic fit to the luminosity function of Soifer *et al.* (Ref. 5):

For $L_{gal} \geq 10^{10.4} L_\odot$,

$$log(\rho_{gal}) = -4.38 - 2.31 \times log(L_{gal}/10^{11} L_\odot), \quad (4a)$$

and for $L_{gal} < 10^{10.4} L_\odot$,

$$log(\rho_{gal}) = -2.08 - 0.65 \times log(L_{gal}/10^{9} L_\odot), \quad (4b)$$

where L_{gal} is the bolometric galaxy luminosity, and ρ_{gal} is the volume density in Mpc^{-3} mag^{-1}. A factor of 0.87 has been applied to Eq. 4 to make the integrated number of galaxies at 0.4 Jy and 60 μm be exactly 0.5 galaxy per deg^2 to match the source density of galaxies in the *IRAS* Point Source Catalog (*e.g.* Ref. 6). The luminosity function is modeled for L_{gal} in the range $10^9 L_\odot$ to $10^{13} L_\odot$, and is set to zero elsewhere.

The spectral energy distribution of each source is a function of its luminosity only, and consists of combinations of 4 thermal components representing cirrus and "starburst" emission, and of a power law component for active nuclei. The parameters defining the components and their combinations were chosen to fit the *IRAS* color-color diagrams (*e.g.* Ref. 7). Galaxies less luminous than $10^{10} L_\odot$ have cirrus-like emission only, with 75% of their luminosity appearing as a 30 K blackbody modified by an emissivity proportional to $\nu^{1.5}$, and the remaining 25% appearing as a 300 K blackbody.

For sources with $10^{10} L_\odot \leq L_{gal} \leq 8\ 10^{12} L_\odot$, the luminosity in excess of $10^{10} L_\odot$ appears as cold and hot starburst components with blackbody spectra carrying 70% and 30% respectively of the excess term $L_{sb} = L_{gal} - 10^{10} L_\odot$, and with temperatures given by $(L_{sb}/10^{11} L_\odot)^{0.1} 60$K and $(L_{sb}/10^{11} L_\odot)^{0.1} 175$K respectively. Finally, luminosity in excess of $8\ 10^{12} L_\odot$ appears as a power-law component with a spectral shape given by $f_\nu \propto \nu^{-0.8}$.

The flux density of a galaxy as seen from the Earth at a frequency ν depends on the luminosity and spectral energy distribution of the galaxy as well as on the assumed cosmology:

$$f_\nu(\nu) = S_\nu(\nu_o) \times (1+z) \left(\frac{d_{ref}}{d_{lum}}\right)^2, \quad (5)$$

where $S_\nu(\nu_o = \nu(1+z))$ is the flux density that would be observed from the galaxy at a cosmologically insignificant distance, d_{ref}. The multiplicative factor of (1+z) accounts for the decreased bandwidth of the observed, as compared to the emitted, radiation. The distance to the galaxy and remaining cosmological effects are given by the luminosity distance, d_{lum}, which is defined as

$$d_{lum} = \frac{c}{H_0 {q_0}^2} [q_0 z + (q_0 - 1)(\sqrt{2q_0 z + 1} - 1)]. \quad (6)$$

The limiting redshift, z_{max}, to which a galaxy of luminosity L can be detected at flux densities greater than f_ν at frequency ν is determined by the implicit solution of Eq. 5 after substitution of Eq. 6.

The surface density of galaxies at a given flux density limit is determined by evaluating the total number of galaxies in each luminosity range out to the limiting redshift $z_{max}(L)$, and integrating over all luminosities. The number of observable sources in a

given volume is a complicated function of distance and cosmology (Eq. 15.3.27 in Ref. 8),

$$N_{gal} = 4\pi H_0{}^{-3} q_0{}^{-4} \int_0^\infty dL \int_0^{z_{max}(L)} (1+z')^{-6} \times (1+2q_0 z')^{-1/2} \left[z' q_0 + (q_0 - 1)(\sqrt{2q_0 z'+1} - 1)\right]^2 \times \rho(z', L)\, dz', \quad (7)$$

where the volume density of galaxies is based on the local luminosity function $\rho(0, L)$ as in Eq. 4,

$$\rho(z, L) = \rho(0, L)(1+z)^{3+\gamma} \quad (8)$$

and the γ in the exponent allows for density evolution. Finally, the surface density is obtained by dividing the total number of galaxies by 4π sr.

Fig. 1 shows the estimated cumulative source densities $N(f_\nu, \nu)$ at two wavelengths, and for two degrees of density evolution, γ =0 and 2, assuming $q_0 = 0.5$ and $H_0 = 100$ km s^{-1} Mpc^{-1}. The effect of the Hubble expansion is evident in the turn-over of the cosmological (relative to Euclidean) source counts at flux densities below the 1 mJy level. In addition, the source counts are affected by the K-correction, which accounts for the dependence of the observed spectral shape on the redshift of the emitting galaxy. At wavelengths shorter than 100 μm the K-correction shifts the extremely weak mid-infrared emission of galaxies into the observing band, thus causing the source counts to fall steeply relative to the Euclidean slope. Longward of 300 μm (on the Rayleigh-Jeans wing of the spectrum), and up to redshifts $z \lesssim (\lambda/150\mu\text{m} - 1)$, the K-correction has the opposite effect, making galaxies easier to detect at greater distances, and enhancing the source counts at a few mJy.

The effect of density evolution with $\gamma = 2$ is to double the source counts at the 1 mJy level. The net result at 300 μm is a dramatic enhancement of the cosmological galaxy density relative to the Euclidean case, then a rapid fall-off at $f_\nu < 1$mJy.

3.2. Estimation of Faint Source Confusion

The source counts $N(f_\nu, \nu)$ can be turned into a faint source confusion noise estimate once two simplifying assumptions have been adopted. First, let all sources be unresolved, and approximate the beam shape by a pill-box function. We can then write the number of sources fainter than f_ν and falling within one beam as $\Omega_{bm} N(f_\nu, \nu)$, and the rms fluctuations in the integrated flux from all these sources as

$$\sigma^2_{conf}(f_\nu) = -\Omega_{bm} \int_0^{f_\nu} f^2 \frac{dN(f)}{df} df. \quad (9)$$

The second assumption is that the source counts can be approximated over the range of flux densities that contributes significantly to the above integral by a power law function of the flux density, namely $N(f_\nu, \nu) = K f_\nu^a$. This simplifies Eq. 9 to

$$\sigma_{conf}(f_\nu) = \left[\frac{-a}{2+a} \Omega_{bm} N(f_\nu)\right]^{\frac{1}{2}} f_\nu. \quad (10)$$

Thus to achieve a fractional photometric accuracy of p, $\sigma_{conf}(f_\nu)$ must be less than $p f_\nu$. The faint source confusion limit is therefore given by the root $f_{\nu,conf}$ of the equation:

$$\left[\frac{-a}{2+a} \Omega_{bm} N(f_\nu)\right]^{\frac{1}{2}} = p. \quad (11)$$

The resulting limiting noise $\sigma_{conf} = p f_{\nu,conf}$ can be meaningfully combined with other noise figures such as detector noise. This statement is based on a comparison of the present formalism with a numerical simulation of the effects of confusion on photometry carried out by George Rieke (Ref. 9, 10).

In our implementation we set $p = \frac{1}{5}$, corresponding to 20% limiting photometry, and searched the source count curves numerically for roots of Eq. 11 starting at large values of f_ν. In all cases the source counts were sufficiently well behaved that roots could be found. For $-3/2 \leq a \leq -1$, those roots correspond to inverse source densities of 75 to 25 beams per source.

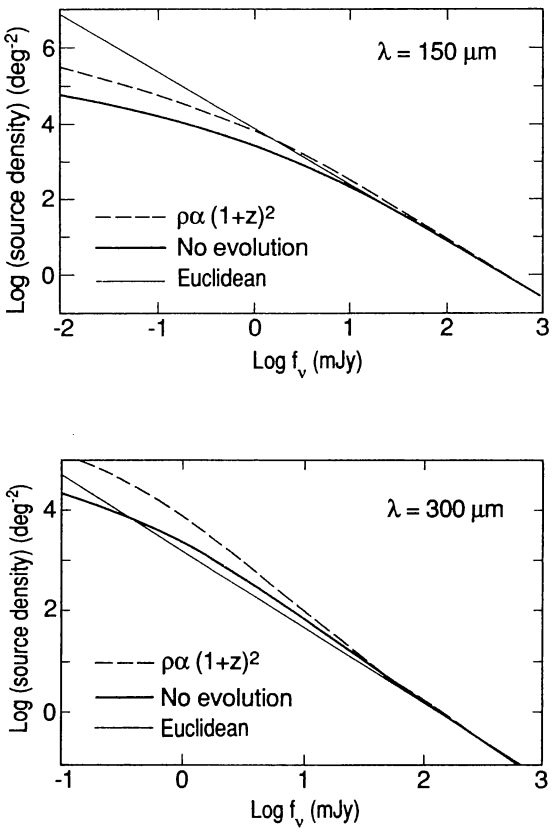

Fig. 1. Cumulative source counts as a function of flux density for 150 μm (upper frame) and 300 μm (lower frame) from our model calculations detailed in §3.1. The dashed curves assume density evolution with an exponent $\gamma = 2$ (Eq. 8), and the thin line provides comparison with the counts expected in a Euclidean universe.

Since we have assumed that the beam size is given by $\Omega_{bm} = 1.6\lambda^2/A$, the confusion noise is an explicit function of wavelength and of telescope aperture only. The estimates of faint source confusion noise are presented below in §4.3.

3.3. Estimation of Bright Source Confusion

The bright source confusion limit depends on the smallest tolerable distance to bright neighboring sources, expressed as the exclusion solid angle, Ω_{ex} and on the highest tolerable frequency of such neighbors, expressed as an incompleteness fraction, I. This confusion limit sets in when $\Omega_{ex}N(f_\nu) = I$. A reasonable assumption is that sources no closer to each other than the radius of the first dark ring in the beam pattern can be readily separated, and therefore do not affect the photometry substantially; this corresponds to $\Omega_{ex} = 3.55\lambda^2/A$. On the other hand, a completeness of 90% at the lowest flux levels is a reasonable expectation, leading to $I = 0.1$. Combining these parameters, we find that the bright source confusion limit sets in at an inverse source density of about 22 beams per source (for a beam solid angle given by $\Omega_{bm} = 1.6\lambda^2/A$).

Using this inverse source density and the source counts, one can derive the flux density $f_{\nu,CONF}$ at which the faintest sources may be extracted without violating the 90% completeness requirement. Unfortunately, this flux density cannot be translated directly into a noise figure, except by assuming that no sources can be extracted below the $p^{-1}\sigma$ level, and defining *ad hoc* $\sigma_{CONF} = pf_{\nu,CONF}$. This last quantity cannot however be combined quadratically with other noise figures, and the overall confusion limit is simply the larger of the faint or bright confusion limits.

Although the faint and the bright source confusion limits tend to be defined in somewhat different circumstances, namely in the study of individual sources for the first, and in surveys for the second, the relative importance of the two can still be assessed in a generic sense. For the assumptions adopted above, we find $[\Omega_{bm}N(f_{\nu,CONF})]^{-1} \simeq 22$, whereas $[\Omega_{bm}N(f_{\nu,conf})]^{-1} \geq 25$ for $a \leq -1$. Faint source confusion therefore dominates as long as $N(f_\nu)$ rises more steeply than f_ν^{-1} with decreasing f_ν. As may be seen from Fig. 1, this remains the case in our source counts down to $f_\nu \lesssim 0.1$ mJy. Virtually all the limiting levels shown here are derived in this regime, and therefore include only faint source confusion. No confusion estimates are shown below the 0.1 mJy levels because the source counts become quite uncertain there; were such estimates to be attempted however, they would definitely have to include the bright source confusion limits.

4. RESULTS AND DISCUSSION

The faint source confusion limit in the absence of any other source of noise is shown in Fig. 2 as a function of wavelength, and is expressed as the equivalent 1σ noise figure in mJy per beam. Curves based on source counts assuming no evolution are plotted as solid lines for five apertures from 0.5 to 8 meters in diameter. The effects of cosmological evolution are illustrated by the confusion limits for 0.5 meter and 4 meter apertures (dashed lines) derived from source counts using a density evolution exponent γ=2 (§3.1 above). Clearly, evolution does little to affect the results for small apertures longward of 100 μm, because the confusing sources are at low redshifts. For a 4 meter aperture however, evolution roughly doubles the confusion limit, since it increases the source counts. The most direct estimates of γ now available, derived from detailed studies of *IRAS* source counts (Ref. 11), point to values in the range 0 to 4 as a conservative choice, if luminosity evolution is not included. The results with $\gamma = 0$ may thus be regarded as lower limits, but otherwise unlikely to be accurate to better than a factor of two, given the assumptions and extrapolations involved.

The dependence of galaxy confusion on D and λ is sufficiently complex that it cannot be expressed in an analytic form to parallel Eq. 3 above. On a flux density scale, the faint source confusion noise rises steeply as the wavelength increases towards 100 μm, then turns over and falls slowly, roughly as $\lambda^{-0.5}$. For λ greater than the turnover value, the confusion noise is roughly inversely proportional to the aperture diameter D, or equivalently $\sigma_{conf} \propto \Omega_{bm}^{0.5}$ at constant λ. This scaling becomes at least three times steeper at the shorter wavelengths. The turn-over wavelength itself increases as D increases, following roughly $\lambda_{crit} \propto D^{1/3}$.

As may be expected from the visibility function, the observed source density in our simulations is dominated by galaxies at the break in the luminosity function at $L^*_{gal} = 10^{10.4}L_\odot$. Moreover, the emission spectrum of these galaxies is constant in their rest-frame since no luminosity evolution is included. λ_{crit} must therefore correspond to the turn-over wavelength of the emission spectrum of L^*_{gal} galaxies shifted by the typical redshift of the confusing galaxies. Thus the doubling of λ_{crit} as the aperture goes from 0.5 to 4m suggests that the typical confusing source at D = 4m is at $z \simeq 1.2$, scaling from $z \simeq 0.1$ for D = 0.5m.

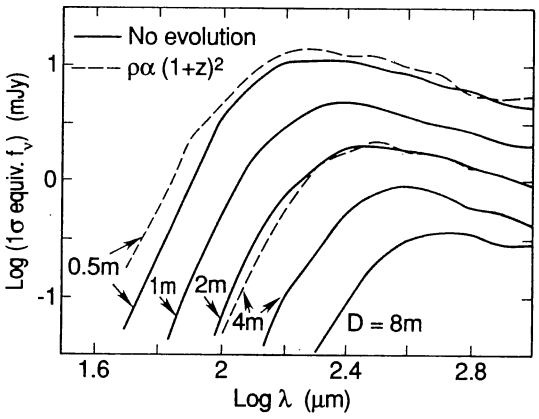

Fig. 2. The estimated noise due only to faint source confusion (§3.2) as a function of wavelength. Each curve is labeled by the aperture diameter D of the telescope, and all observations are assumed to be made with a detection element with an angular diameter $1.6\lambda/D$. The dashed curves have the same meaning as in Fig. 1. Ripples on curves are due to numerical approximations. See §4 for more details.

At constant aperture D, significant gains can be made against all sources of confusion by sampling at greater spatial frequencies, as opposed to the assumption here that observations are made through an aperture $\Omega_{bm} = 1.6\lambda^2/D$. Faint source confusion would be reduced because of the smaller effective number of sources per detection element. The decrease in bright source confusion arises from the increased ability to deconvolve close neighbors. The achievable improvement probably peaks near a factor of three in σ_{conf} since diffraction will always couple the information in neighboring elements; increasingly finer spatial sampling eventually renders our formalism inapplicable. The Multiband Imaging Photometer for SIRTF has opted for over-sampling in the spatial domain specifically to fight confusion at $\lambda > 100$ μm.

5. COMPARISON OF NOISE SOURCES

Fig. 3 shows estimates for three noise sources for a 1 meter cryogenic telescope, similar in design to ESA's Infrared Space Observatory (ISO) or NASA's Space Infrared Telescope Facility (SIRTF). Such an instrument has its optics cooled by liquid Helium to avoid thermal background noise, and uses state-of-the-art detectors in the focal plane, thus achieving a sensitivity limited only by the celestial backgrounds. The cryogenic design of such telescopes limits their sizes to about one meter, thus leaving them susceptible to confusion noise. The solid lines in Fig. 3 show the faint source confusion noise. The dashed lines show the cirrus confusion noise expected in an area of the sky with a mean brightness of $B_0(100\mu m) = 1.3$ MJy sr^{-1}. About 10% of the sky may be expected to be fainter than this level, based on the statistics in Boulanger and Pérault (Ref. 2). The dotted lines represent the remaining noise sources after 1000 seconds of integration, arising from a combination of detector and photon noise (both telescope and celestial backgrounds), assuming the proposed SIRTF complement of detectors: For $\lambda < 200\mu$m, photoconductors with an efficiency of 0.15, a dark current of $1.8(\lambda/1\mu m)^{1.2}e^-s^{-1}$, and a read current of $40e^-$; and for $\lambda > 200\mu$m, bolometers with an efficiency of 0.5, and a noise-equivalent power of 5 10^{-17} W Hz$^{-1/2}$. The thermal background from the optics is modelled as a 5 K greybody with 50% emissivity, and the observations are assumed to use a bandwidth $\Delta\lambda = \lambda/3$. Two sets of curves are given, one labeled **A** assuming $\Omega_{bm} = 1.6\lambda^2/A$, and the other labeled **B** assuming smaller detection elements with $\Omega'_{bm} = 0.64\lambda^2/A$, corresponding to $d' = \lambda/D$. As expected, the enhanced spatial sampling achieves a threefold improvement in cirrus confusion noise, and cuts in half the galaxy confusion noise.

It can immediately be seen that cryogenic apertures of one meter or less will be severely confusion limited longward of 200 μm, with faint sources becoming more important than cirrus in about 10% of the sky, and *vice versa* elsewhere. Because of the steepness of the confusion curves around 100 μm, the precise cross-over wavelength at which confusion rises to dominance will depend sensitively on the parameters of instrumental configuration and of the astrophysics which enter the modeling.

Fig. 4 addresses a four-meter aperture, passively cooled in space, similar in concept to missions like ESA's Far Infrared and Submm Telescope (FIRST), or NASA's Sub-Millimeter Imaging and Line Survey (SMILS). With an assumed temperature of 150 K, an emissivity of 20%, and an observing bandwidth $\Delta\lambda = \lambda/3$, the thermal background from the optics completely determines the photometric performance of such a telescope, for bolometers with an intrinsic noise equivalent power of 2 10^{-16} W Hz$^{-1/2}$, and an efficiency of 80%. Even at its maximum, faint source confusion will not be a problem for integrations lasting less than an hour. The dashed line in Fig. 4

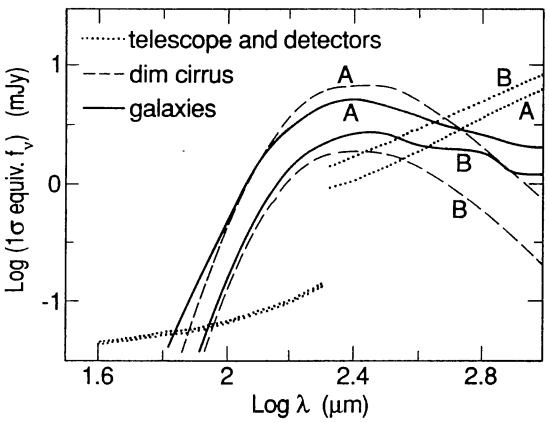

Fig. 3. Comparison of estimated levels of noise (after 1000 seconds of integration) from three different sources for a one-meter cryogenic telescope, operating with a beam diameter of either $1.6\lambda/D$ (curves labeled **A***), or λ/D (curves labeled* **B***). The dotted curves include photon noise from the telescope emission as well as celestial backgrounds. See §5 for more details.*

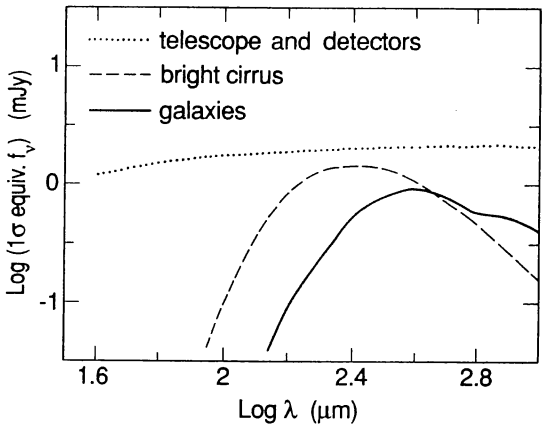

Fig. 4. Comparison of estimated levels of noise (after 1000 seconds of integration) from three different sources for a four-meter passively cooled telescope in Earth orbit, operating with a beam diameter of $1.6\lambda/D$. The dotted curve is dominated by photon noise due to thermal emission from the telescope. See §5 for more details.

shows the expected cirrus confusion noise in an area with $B_0(100\mu m)$=4.5 MJy sr^{-1}, which is the mean brightness of the sky at a Galactic latitude near 30°. Cirrus confusion and faint source confusion peak at different wavelengths for a 4-meter aperture. Because the first of the two decreases faster with increasing aperture diameter, they are comparable in flux density in relatively bright cirrus, as opposed to the 1-meter aperture case (Fig. 3).

Thus confusion by extragalactic sources will enter the picture for a 4 meter or larger aperture only for long integration times (more than an hour). Though peaking at a different wavelength, it will surpass cirrus confusion in magnitude over only half the sky.

6. SUMMARY AND CONCLUSIONS

We have modeled the emission from galaxies to estimate extragalactic source counts at infrared and submm wavelengths, and derived the associated confusion limits for photometric observations using telescopes of various sizes. The limits due solely to this type of confusion amount to $\lesssim$10 mJy for $\lambda >$ 150μm for a 0.5 meter aperture, and $\lesssim$1 mJy for $\lambda >$ 300μm for a 4 meter aperture, assuming a detection element of solid angle $\Omega_{bm} = 1.6\lambda^2/A$. At wavelengths shorter than those turn-over values, confusion drops off quickly, and at longer wavelengths it varies roughly like $\lambda^{-0.5}$. Including cosmological density evolution in modeling the galaxy population will not affect the results for the 0.5 meter telescope, but will double the noise estimate for the 4 meter aperture. Sampling the sky at finer spatial resolution than Ω_{bm} above could easily cut the confusion noise in half.

We have extended the work at 100 μm by Gautier *et al.* (Ref. 3) to estimate confusion by cirrus at all wavelengths, and find the following approximation:

$$\frac{\sigma_{cir}}{1\mathrm{mJy}} \simeq 0.3 \left(\frac{\lambda}{100\mu\mathrm{m}}\right)^{2.5} \left(\frac{D}{1\mathrm{m}}\right)^{-2.5} \left(\frac{B_0}{1\mathrm{MJysr}^{-1}}\right)^{1.5} \quad (12)$$

where B_0 is the local mean brightness of cirrus.

In comparing the confusion estimates to models of typical space-borne telescopes proposed for the far infrared and submm, we find that cirrus confusion would outweigh extragalactic source crowding over 90% of the sky for a 1 meter aperture. Cryogenic telescopes in the one meter class would be dominated by confusion at $\lambda \gtrsim 100\mu$m for integration times longer than a few minutes (assuming sufficiently sensitive detectors). The majority of confusing sources would reside at redshifts between 0.1 and 0.2.

A four-meter passively cooled aperture however would not reach the sensitivity limits which expose it to confusion by galaxies until at least an hour of integration. The confusing sources would typically reside at redshifts between 1 and 3/2. For a four-meter aperture, cirrus is less significant than galaxies as a source of confusion over half the sky.

The above estimates are based on rather daring extrapolations from *IRAS* data; much more data are needed, especially at $\lambda > 100\mu$m, to improve the assumptions and the estimates. While cirrus and galaxies were viewed here as "noise", they figure as "signal" in the study of Galactic structure and cosmology. The fact that cryogenic telescopes are limited by confusion after short integration times implies that these will be powerful instruments in the study of cirrus and of extragalactic sources.

It should also be stressed that the typical redshift of confusing sources is by no means the largest redshift that an instrument can usefully probe: The *IRAS* bright galaxy sample of Soifer *et al.* (Ref. 5), complete for $f_\nu(60\mu m) \geq 5.24$Jy, has a median redshift of 0.008, yet more than 10% of its sources are at redshifts greater than 0.025.

We would like to thank Jean-Loup Puget and George Rieke for stimulating discussions and significant suggestions, and Mary-Ellen Barba for help with the manuscript. The Astronomy Department at Cornell graciously hosted G.H. during part of this work. This research was supported through the *IRAS* Extended Mission Program by the Jet Propulsion Laboratory, California Institute of Technology, under contract with the National Aeronautics and Space Administration.

REFERENCES

1. Low F J *et al.* 1984, Infrared cirrus: new components of the extended infrared emission, *Ap J (Letters)*, **278**, L19.
2. Boulanger F and Pérault M 1988, Diffuse infrared emission from the Galaxy. I. Solar neighborhood, *Ap J*, **330**, 964.
3. Gautier T N III, Boulanger F, Pérault M and Puget J-L 1990, A calculation of confusion noise due to infrared cirrus, *A J*, in press.
4. Désert F-X, Boulanger F, and Puget J-L 1990, Interstellar dust models for extinction and emission, *A & A*, in press.
5. Soifer *et al.* 1987, The *IRAS* bright galaxy sample, *Ap J*, **320**, 238.
6. Soifer, B T, Houck, J R, and Neugebauer, G 1987, The *IRAS* View of the Extragalactic Sky, *Ann Rev A & A*, **25**, 187.
7. Rowan-Robinson M, and Crawford J 1986, Models for *IRAS* galaxies, in *Light on Dark Matter*, ed. F P Israel (Dordrecht: Reidel) p. 421.
8. Weinberg S, 1972, Gravitation and cosmology (New York: John Wiley and Sons).
9. Rieke G H 1987, Calculations of SIRTF sensitivity at 40 to 300 μm (Rev. B), preprint.
10. Rieke G H, Beichman C A, and Gautier T N 1988, Natural limits to far infrared observations, *B A A S*, **20**, 1096.
11. Lonsdale C J, Hacking P B, Conrow T P and Rowan-Robinson M 1990, Galaxy evolution and large-scale structure in the far-infrared. II. The *IRAS* faint source survey, *Ap J*, **358**, 60.

Discussion - Paper II.11.

Q - D.B. SANDERS : Do you have an estimate of at what redshift the galaxies lie where galaxy confusion sets in ?

A - G. HELOU : The bulk of the confusion is contributed by galaxies at L^* in the luminosity function. For a 4 meter telescope, these are at a redshift of 1 or so. It is important to remember however that the telescope could still detect galaxies at redshifts higher than 1, even though it is confused by galaxies at z = 1.

Q - C. MASSON : Did you allow for clustering of galaxies in your calculations ?

A - G. HELOU : No, we have assumed the galaxy population to be uniformly distributed on the sky.

C - R. HILLS : The good news about the confusion is that one is going to find lots of objects by searching a modest number of beam areas. The problem is whether or not they will be interesting objects.